Friction **8**(5): 893–904 (2020)
https://doi.org/10.1007/s40544-019-0306-2
ISSN 2223-7690
CN 10-1237/TH
RESEARCH ARTICLE

Exploring the friction and wear behaviors of Ag–Mo hybrid modified thermosetting polyimide composites at high temperature

Chunjian DUAN[1,2], Ren HE[3], Song LI[1,2], Mingchao SHAO[1,2], Rui YANG[1,2], Liming TAO[1], Chao WANG[1], Ping YUAN[3], Tingmei WANG[1,*], Qihua WANG[1,*]

[1] *State Key Laboratory of Solid Lubrication, Lanzhou Institute of Chemical Physics, Chinese Academy of Sciences, Lanzhou 730000, China*

[2] *University of Chinese Academy of Sciences, Beijing 100049, China*

[3] *Institute of System Engineering, China Academy of Engineering Physics, Mianyang 621900, China*

Received: 10 January 2019 / Revised: 15 April 2019 / Accepted: 30 May 2019

Abstract: Polyimide composites have been extensively used as motion components under extreme conditions for their thermal stability and special self-lubricating performance. In the present study, Ag–Mo hybrids as lubricant fillers were incorporated into thermosetting polyimide to prepare a new type of tribo-materials (TPI-1) at high temperature. Comprehensive investigations at different temperatures reveal that the newly developed TPI-1 exhibits a better reduction in friction and wear rate below 100 ℃, but all of them increase significantly when the bulk temperature exceeds 250 ℃. The wear mechanisms demonstrated that sandwich-like tribofilms with different layers were established at different temperatures, which was further verified by characterization of scanning electron microscope (SEM), Raman spectroscopy, and transmission electron microscope (TEM). Considering the high-performance TPI coupled with Ag–Mo hybrids, we anticipate that further exploration would provide guidance for designing TPI tribo-materials that would be used at high temperatures.

Keywords: polyimide; Ag–Mo hybrids; self-lubricating composites; high temperature tribology

1 Introduction

The lifespan of many types of machinery is dependent on tribo-materials. Reduction in friction and wear is not only beneficial to energy conservation, but also provides economic benefits by preventing unnecessary maintenance [1]. Self-lubricating polymer-matrix materials demonstrate their potential by replacing some important parts previously made from metal, such as bearings, seals, and so on [2–6]. With rapid developments in science and technology, the application conditions for self-lubricating polymer composites will become more demanding for special requirements in space, such as extremes of both high and low temperatures and high vacuum [7]. The choice of polymer materials which could be used under a wide range of temperatures is currently limited. With excellent mechanical properties, remarkable heat-resistance and self-lubrication, thermosetting polyimide (TPI) has attracted the attention of researchers in designing lubricating materials [8–13].

However, TPI self-lubricating composites with better wear resistance and lower friction at high temperature is still a challenge. In the search for effective lubricants, numerous studies have been undertaken at room temperature [14–16]. Many results have shown that polymers with 2D solid lubricants are beneficial informing tribofilms on mating surfaces, and the intrinsic ease of shearing of these materials resulted in friction reduction [17–21]. Another frequently studied

* Corresponding authors: Tingmei WANG, E-mail: wangtin3088@sina.com; Qihua WANG, E-mail: wangqh@licp.cas.cn

concept is to enhance load bearing and reduce abrasion by incorporating various fibers and metal oxide nanoparticles [5, 22, 23]. The friction and wear behavior of TPI composites at high temperature is different from room temperature, but this work has been rarely reported at [24, 25]. To the best of our knowledge, this phenomenon may be due to two reasons: the intrinsic conflict for TPI between high heat-resistance and the molding process, and the difficulty in obtaining suitable solid lubricants [26]. As is well known, the lubricating properties of numerous solid lubricants, such as graphite, molybdenum disulfide (MoS_2), and others, are rapidly degraded at elevated temperatures [27]. It is therefore essential to provide TPI with a suitable solid lubricant which can be used at high temperature. Inspired by "chameleon" surface adaptation, soft and ductile silver and molybdenum are frequently introduced as solid lubrication at high temperature [28, 29]. The mechanism of lubrication is provided by silver at lower temperature and the further formation of a series of oxides between silver and molybdenum at higher temperature [30–32]. Moreover, from the Archard wear equation ($Q = KWL/H$, where Q is wear volume, K is a constant, W is load, L is the sliding distance), and H is the hardness of material, high hardness of the molybdenum phase can also endow TPI composites with better wear resistance at high temperature. On the basis of the above analyses, we wished to investigate whether they could provide TPI with effective lubrication below 400 ℃. As far as we know, exploration in this area has not been reported previously. Moreover, wear mechanism which is primarily dependent on tribo-chemical reactions cannot be measured over time due to the difficulty in measuring the temperature on the worn surface. In view of this problem, the question arises whether it is possible for us to make use of these products generated at different temperatures as indicators to indirectly infer the actual temperature on worn surfaces, as demonstrated in Ref. [33]. That study is a meaningful attempt to estimate actual temperature with a series of oxides between silver and molybdenum during friction.

In this study, we successfully prepared TPI composites with Ag-Mo hybrids and two different reinforced fibers which were used to enhance the load-carrying capacity of the polymer matrix. The friction and wear behavior of TPI composites were systematically investigated at different temperatures. The morphologies of the wear track and counterpart were characterized to understand the lubricating effects of Ag-Mo hybrids, and the evolution of dominant wear mechanisms of the TPI composites was revealed in relation to the microstructure of the worn surface.

2 Materials and methods

2.1 Materials

TPI with a $T_g \approx 320$ ℃ was synthesized according to our previous work. The detailed synthesis method was reported in Ref. [34]. Aramid pulps and carbon fibers (length: 10–20 mm, the diameter: 7 μm) were supplied by Shanghai Teijin Aramid Ltd., China, and Nantong Senyou Carbon Fiber Co., Ltd., China, respectively. The molybdenum and Ag were purchased from Tianjin Kemiou Chemical Reagent Co., Ltd., China.

2.2 Preparation of TPI composites

The composites were prepared with the conventional method of hot press molding. In order to improve the interfacial adhesion between the fiber and the matrix, the commercial fibers were soaked in acetone for 24 h, and then cleaned using anultrasonic cleaner (SK8200, high-frequency ultrasonic model, China) for 0.5 h. It was then dried at 100 ℃ before using.

In order to achieve sufficiently reaction between Ag and Mo during friction, Ag–Mohybrids were initially prepared by simply mixing Ag and Mo with alcohol (> 99.6%). Thereafter, all ingredient materials were soaked in alcohol (> 99.6%) and mixed in a high-speed blender (DFY-250C, Linda machinery Co., Ltd., China) at a rotation speed of 12,000 rpm with an ultrasonic bath. After being dried for approximately 24 h at 100 ℃, the mixture was compressed in a mold (45 mm × 60 mm) with a pressure of about 10 MPa for 30 min and then heated up to 375 ℃ at a rate of 5 ℃/min with intermittent deflation. The pressure was held at 20 MPa for 120 min to allow a full compression sintering. Detailed compositions, hardness (HV), and densities (ρ) of the composites are listed in Table 1.

Table 1 Chemical compositions of TPI composites.

Code	Ag (wt%)	Mo (wt%)	Carbon fiber (wt%)	Aramid pulp (wt%)	HV (MPa)	ρ (g/cm^3)
TPI	0	0	0	0	20.3 ± 0.6	1.24
TPI-1	10	5	5	10	30.1 ± 2.3	1.43

2.3 Tribological tests

Tribological tests were measured at different temperatures in ambient air on a ball-on-disk tribometer (CSEM-THT07-135, Switzerland). A schematic of the contact can be seen anywhere [34]. A steel ball bearing (GCr15, GB/T 18254-2016) was used as a counterpart. A circular movement with a radius of 5 mm was applied under normal force (F) 5 N and velocity (V) 0.1 m/s. Temperature of RT, 50, 100, 200, 250, 300, and 350 ℃ were applied and each test was repeated at least three times. The wear rate (WR) was calculated according to the following formulae:

$$\Delta V = \left[\frac{\pi\left(\frac{R}{2}\right)^2}{180} \sin^{-1}\left(\frac{b}{R}\right) - \frac{b\sqrt{\left(\frac{R}{2}\right)^2 - \left(\frac{b}{2}\right)^2}}{2} \right] \cdot \pi d \quad (1)$$

$$K = \frac{\Delta V}{PL} \quad (2)$$

where ΔV is the wear volume (mm^3), K is the specific wear rate (mm^3/(N·m)), R is the diameter of the bearing steel ball (3 mm), b is the width of the wear trace (measured with a surface mapping profiler), d is the diameter of the circle (10 mm), L is the sliding distance in total (m), and P is applied load (N).

2.4 Characterization

The size and morphology of different samples were inspected by a Malvern 3000 laser diffraction analyzer (Malvern, UK) and a field emission scanning electron microscope combined with energy dispersive spectrometer (FE-SEM/EDS). The FE-SEM/EDS was also employed to characterize the worn surfaces and tribofilms formed on the counterpart and the cross-section of TPI-1 composites. The possible tribochemical reactions between TPI-1 and the counterpart were analyzed using Raman spectroscopy and X-ray diffraction (XRD). In addition, a cross-sectional area of tribofilms lamellae was prepared by focused ion beam (FIB, FEI Quanta 3D, the Netherlands) and the nanostructures were examined with high resolution transmission electron microscopy (HR-TEM, Tecnai G2 TF20 S-TWIN) equipped with energy dispersive X-ray spectroscopy (EDXS). To further understand the crystal structure in the tribofilms where we are interested, selected area electron diffraction (SAED) was used simultaneously for in-depth inspection.

3 Results and discussion

3.1 Microstructures and cross sections of TPI composites

The SEM images of the Mo and Ag nanoparticles are shown in Fig. 1. It appears that all powders present spheroidal shapes or irregular rods. From the size distribution curves, it can be seen that the size of Mo particles is in the range of 1−100 μm (Fig. 1(a1)), but the particle size distribution of Ag is in the ranges between 7−20 nm and 1−100 μm. The Mo micro-sized particle gave rise to a connection with Ag in the nano-sized particle range and may lead to more possibility of chemical reactions between them during the process of friction. The XRD patterns of Mo-Ag hybrid modified TPI composite are shown in Fig. 7(b). The TPI composite mainly consists of amorphous phase (broad peak about 2θ = 23°), which would be attributed to TPI. The single phase of Ag and Mo was also detected in TPI-1 with any other new phases (JCPDS No.65-8428 and JCPDS No.42-1120) [28]. It demonstrated that the Ag and Mo were not oxidized in the TPI matrix during the heat-pressing process.

An SEM micrograph of the TPI-1 cross-section is shown in Fig. 2(a). From its brittle fracture morphology with little scaly appearance, we can infer that the nanoparticles of Ag and Mo are not well bonded with the TPI matrix. In order to detect dispersion of the fillers, EDS analysis was conducted on the cross-section. As illustrated in Figs. 2(b)−2(f), homogeneous distribution

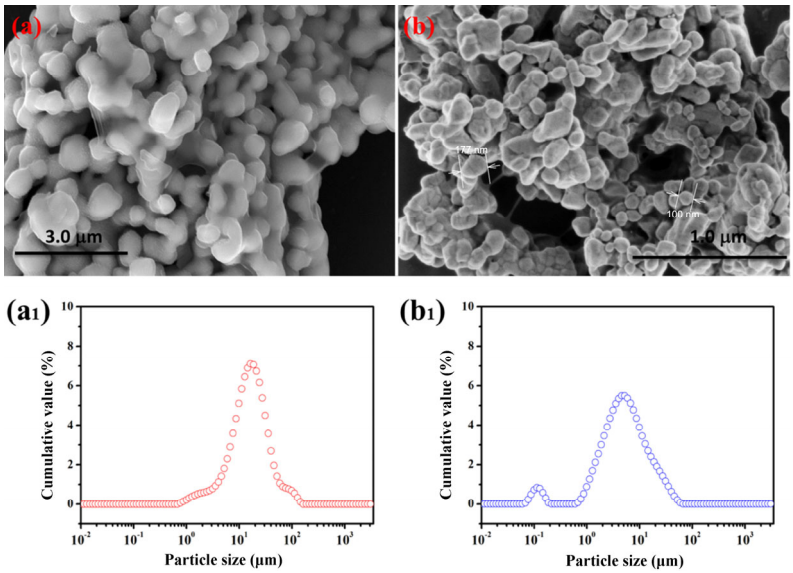

Fig. 1 SEM morphologies and particles size distribution of ((a) and (a1)) molybdenum and ((b) and (b1)) silver.

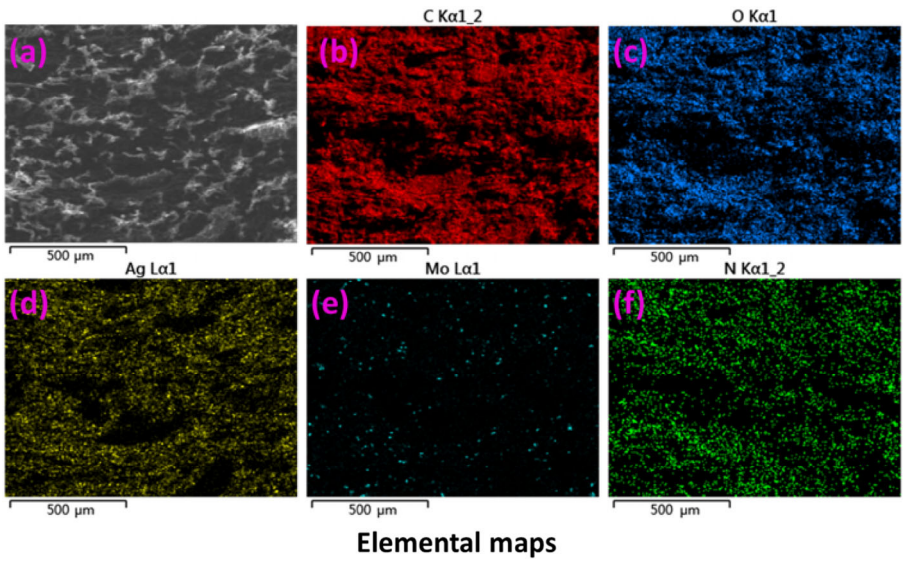

Fig. 2 (a) SEM micrographs of TPI-1 cross-section and its EDS maps of elements: (b) C, (c) O, (d) Ag, (e) Mo, and (f) N for TPI-1.

of the elements for C, N, O, Ag, and Mo verified that all of the fillers were well dispersed in the TPI matrix.

3.2 Friction and wear properties

The friction and wear behavior of TPI-1 are comparatively investigated at different temperatures and the results are shown in Fig. 3. As shown in Fig. 3(a), the coefficient of friction (COF) with sliding distance can be divided into two parts as a function of temperature: 1) At lower temperatures (below 100 ˚C), a lower steady-state COF is established after slightly increasing; and 2) at higher temperatures (above 200 ˚C), a higher steady-state COF was observed with an obvious stick-slip (apart from 250 ˚C). In Fig. 3(b), the average of COF and wear rate are shown from room temperature to 350 ˚C. According to our previous work, pure TPI exhibits a high COF (above 0.6) at lower temperatures [34]. However, for the TPI composites modified with Ag-Mo hybrids, it shows a lower COF of about 0.34 from RT to 100 ˚C. We believe that the COF is closely connected with orientation effects of the TPI molecular chain. Higher temperature and friction-induced shear activate the molecular chains

and result in reorientation with the sliding direction [24]. In contrast with the pure TPI, it is interesting to find that the COF of TPI composites rises to about 0.56 by incorporation of Ag–Mo hybrids at 200 ℃. This may be due to the presence of abundant wear debris stripped from broken molecular chains or fillers. When the bulk temperature increases to 250 ℃, it reaches its lowest value of about 0.24 after the wear debris is compacted and forms more uniform tribofilms. After the temperature is increased above 250 ℃, the COF is more dependent on different fillers and sharply increased. The variation of WR for TPI-1 is consistent with the COF at different temperatures. As shown in Fig. 3(b), the WR is in the range of 4.5×10^{-6}–7×10^{-6} mm^3/(N·m) below 100 ℃. When the temperature reached 200 ℃, WR increased by at least one order of magnitude (2.47×10^{-5} mm^3/(N·m)), which also verifies our inference regarding the sharp increase in the COF. As the temperature increased above 250 ℃, the largest value of wear rate was observed at 350 ℃, which was 6.4×10^{-5} mm^3/(N·m). In comparison to the pure TPI, it can be concluded that TPI with Ag-Mo hybrids possesses good tribological properties at lower temperature, especially below 100 ℃.

3.3 Structures of tribofilms and worn surfaces

Figure 4 displays the SEM images of worn surface with TPI-1 at different temperatures. As shown in Figs. 4(a)–4(c), some scratches were seen as expected for the high-hardness phase (Mo or its oxide, cf. corresponding EDS analyses in Fig. 5(h)), and large amounts of wear debris and plastic deformation are also detected on the worn surface. It is noted that abrasive wear is the main wear mechanism in this

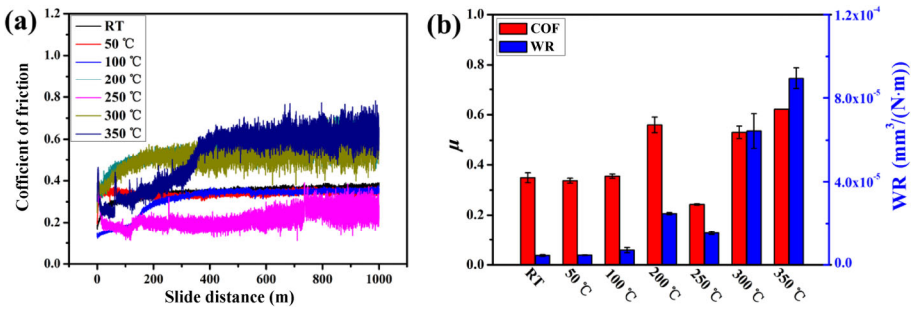

Fig. 3 The measurements for COF and WR of TPI-1: (a) COF as function of sliding distance, (b) the average of COF and WR at different temperatures.

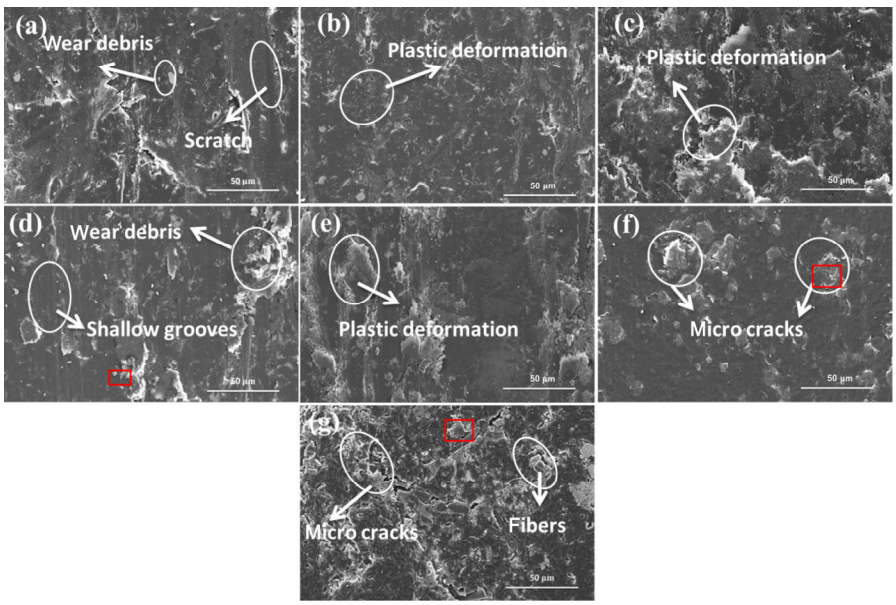

Fig. 4 SEM images of the worn surfaces at (a) RT, (b) 50 °C, (c) 100 °C, (d) 200 °C, (e) 250 °C, (f) 300 °C, and (g) 350 °C.

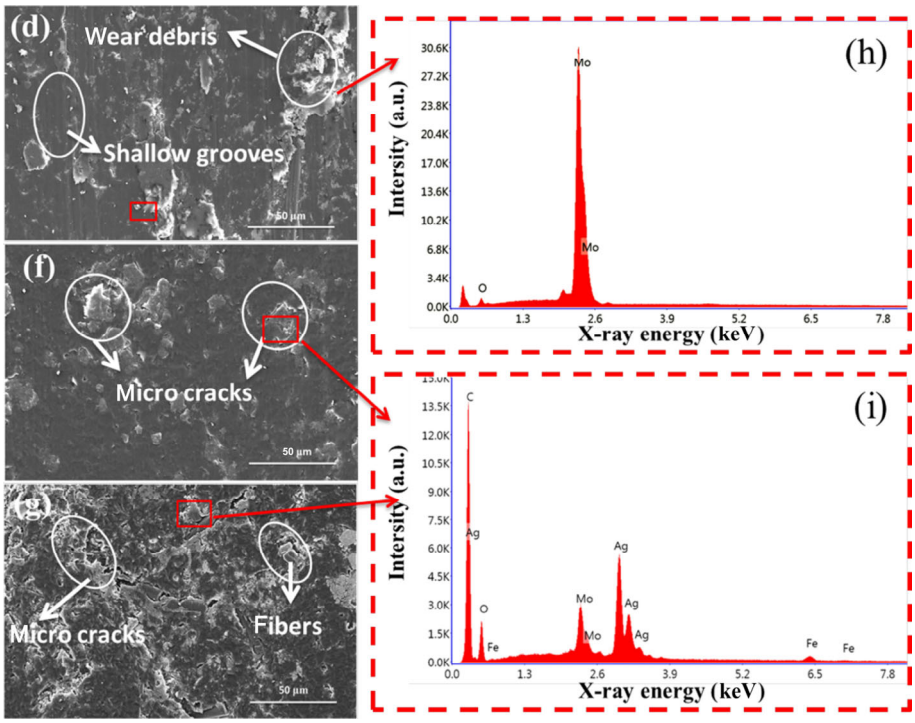

Fig. 5 (h) and (i): EDS analyses of the transfer films formed on GCr15 at different temperatures.

stage. When the temperature is increased above 100 ℃, the worn surface becomes much smoother and wear debris is considerably decreased. Shallow grooves are observed at 200 ℃, ascribed to exposed fillers and accumulation of wear debris (Fig. 4(d)). This consequently caused high friction and abrasion. At 250 ℃, the compacted wear debris and obvious plastic deformation are consistent with a lower COF and WR, and the main wear mechanism becomes adhesive wear (Fig. 4(e)). As shown in Figs. 4(f) and 4(g), many micro cracks are also observed as the temperature is elevated to 300 ℃, and a clear phase separation occurs at 350 ℃. This result allows us to infer that the phase separation is caused by two different phenomena: high thermal diffusion of Ag-Mo hybrids on the worn surface, and the reinforced fibers stripped by reciprocating shear.

EDS results also verify the presence of Ag-Mo hybrids and reinforced fibers near the micro cracks (cf. Fig. 5(i)). In addition, a small amount of Fe is also involved in worn surface (cf. Fig. 5(i)). These results clarify the severe abrasion of TPI-1 at higher temperatures (cf. Fig. 3(a)).

In order to evaluate the mechanism of friction and wear in more detail, typical counterpart surfaces of TPI-1 were examined as shown in Fig. 6. As seen from Fig. 6(a) (RT), an early smooth and continuous tribofilm formed on the steel surface and a little wear debris remained along the slide direction. This is believed to be the main reason for the lower COF of TPI-1 compared with pure TPI (cf. Fig. 3(a)). However, Fig. 6(b) indicates that a non-continuous tribofilm covered with many wear debris formed at 200 ℃, which is consistent with the higher COF and WR. As demonstrated by EDS analyses (Figs. 6(d)–6(i)), it is verified that the broken TPI molecules encountered with Ag-Mo hybrids help to form a tribofilm at 200 ℃. When the temperature increased to 350 ℃, a rough transfer film with furrows without any wear debris is formed on the worn surface (Fig. 6(c)). The above results demonstrate that both the thermal diffusion of Ag-Mo hybrids and the plastic deformation of TPI are beneficial to tribofilm formation at elevated temperatures (cf. Figs. 4(c) and 4(e)).

Figure 7(a) shows the Raman spectra of tribofilms with TPI-1 formed at different temperatures. The fingerprint of Ag_2MoO_4 (895 cm^{-1}) is identified from the spectrum of steel surface at different temperatures, which verifies that the tribo-oxidation of Ag-Mo hybrids has occurred during the friction process [35]. As we know, silver molybdate phase formation is

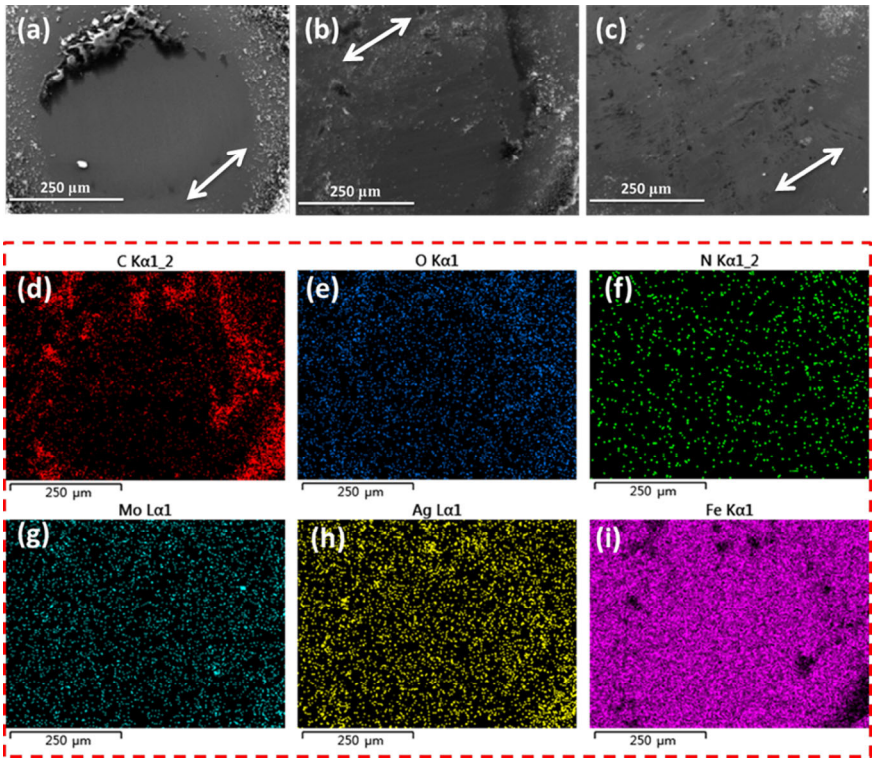

Fig. 6 SEM images of the tribofilms generated at different temperature (arrows is sliding direction): (a) RT, (b) 200 °C, (c) 350 °C, and EDS elemental maps of tribofilms at 200 °C (d)−(i).

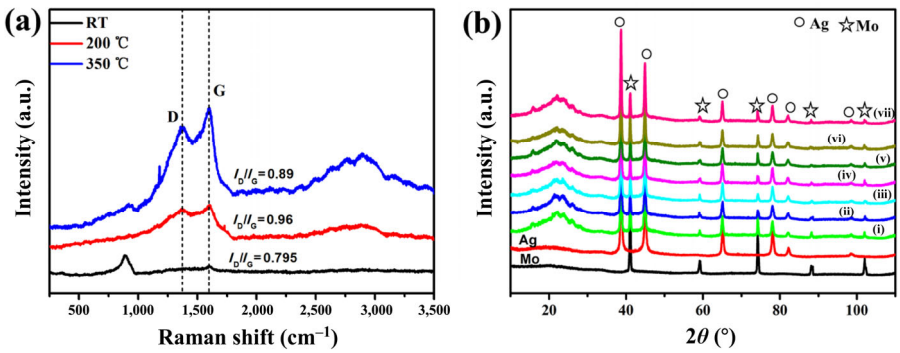

Fig. 7 (a) Raman spectra of steel surface at RT, 200 °C, and 350 °C, (b) XRD patterns of Ag and Mo particles, and worn surface of TPI-1 from RT to 350 °C (i−vii).

closely related to the activity of the high surface area of nano-Ag and Mo on a worn surface [36]. In addition, the peak at lower temperatures is more intense than that at higher temperatures, which is consistent with the better friction and wear behavior of TPI-1 (cf. Figs. 3 and 6). Moreover, D band (1,365 cm^{-1}) and G band (1,593 cm^{-1}) can be found at different temperatures. This observation indicates that carbon materials which would peel from TPI or reinforced fibers are transferred onto the steel surface. In addition, the intensity ratio of D band to G band (I_D/I_G) can also reflect the degree of defects of carbon materials [37, 38]. In comparison to the I_D/I_G ratios at different temperatures (RT: 0.795, 200 ℃: 0.96, 350 ℃: 0.89), it was revealed that carbon materials had a different structure in the tribofilms. Compared with a tribofilm at lower temperatures, structures of carbon show more disorder and defects at higher temperatures. This result is also verified by the high intensity of the D+G peak which is observed at a broad peak in the Raman spectra around 2,800–2,900 cm^{-1} [39]. Although no proof is provided, we believe that chemical reactions

of Ag-Mo hybrids, rather than TPI or transfer, play a dominant role in reduced friction and wear.

Figure 7(b) illustrates the XRD results of worn surface after friction tests at different temperatures. It is worth noting that the diffraction peaks of Ag and Mo, but not of any impurity phases can be simultaneously observed in the TPI-1 at different temperatures. This implies that the silver-molybdenum oxide do not form or cannot be detected. More interestingly, these results are contrary to the Raman analysis of tribofilms of steel surfaces. Although the EDS elemental maps display (cf. Fig. 5) the presence of O, Ag, and Mo on the worn surface, it is difficult to demonstrate the existence of silver-molybdenum oxide. The worn surfaces at different temperatures were therefore inspected using a Raman spectrometer. Contrary to our expectation, Raman peaks below 1,000 cm^{-1} which belong to metallic oxide are not observed. This can be partly ascribed to the oxidation products interspersed at random (the data are not displayed). In fact, it is not feasible to use silver-molybdenum oxide as an indicator to reflect the actual temperatures attained.

On the basis of the above analyses, we speculated that the mechanism of tribofilm formation is closely connected with the large diffusion coefficient and high mobility of Ag and Mo. Taking into consideration the role of Ag-Mo hybrids,a schematic model of sandwich-like tribofilms is offered at high temperatures (Fig. 8). To our best knowledge, the oxidation of steel surfaces is inevitable during the rubbing process. This is followed by easy diffusion of Ag and Mo into the matrix of TPI-1 both vertically and/or horizontally to the worn surface [30, 31]. After reciprocating stress and thermally driven, Ag and Mo are transferred to the counterpart and further oxidize, with the final product being the Ag_2MoO_4 on the steel surface. Finally, the tribofilms of Ag_2MoO_4 are covered with stripped TPI or even partly broken reinforced fibers. It is reasonable to anticipate that the formation of sandwich-like tribofilms could contribute to poor thermal conductivity of the polymer and heat exchange in the vertical direction on the worn surface. On the contrary, TPI or reinforced fibers are more readily deposited at first onto the steel surface and Ag and Mo are more likely to transfer and oxidize at lower temperatures. This is the reason why the COF and WR display a better

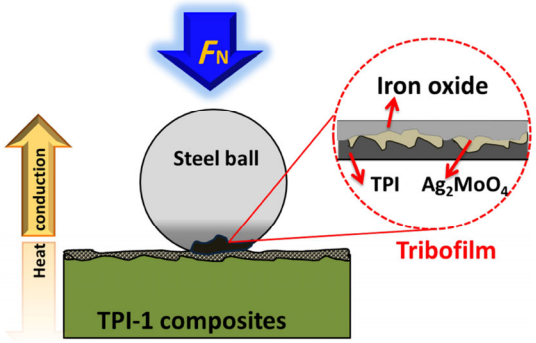

Fig. 8 Schematic of sandwich-like tribofilms formation at higher temperature on the steel surface.

tribological performance at lower temperature. This model can also be verified by Raman analysis showing the appearance of Ag_2MoO_4 at different temperatures.

To further demonstrate this concept, a cross-section of tribofilm formed at 200 ℃ was analyzed by TEM. As shown in Fig. 9(a), it is clear that a robust tribofilm formed on the steel surface with a thickness of approximately 500 to 1,000 nm. Figures 9(b1) and 9(c1) (HR-TEM of regions b and c which are marked in Fig. 9(a)) indicate that the steel surface was oxidized and formed a continuous iron oxide layer according to EDXS analyses (Fig. 9(b3)) [40, 41]. Moreover, most of the amorphous phase (gray phase in Figs. 9(b1) and 9(c1)) and the short-range-ordered phase (black phase in Figs. 9(b1) and Fig. 9(c1)) are observed above the tribo-oxidation layer. From the insets in Fig. 9(c1), fast Fourier transform analyses verify that the short-range-ordered phase belonged to Ag_2MoO_4 corresponding to an interplanar spacing of 0.235 nm (JCPDS No.08-0473). SAED patterns of zone b also corroborate clear diffraction spots of Ag_2MoO_4, which correspond to lattice planes $(3\bar{1}\bar{1})$ and (400) (Fig. 9(b2), JCPDS No.08-0473). Most of amorphous phase probably consisted of the residual TPI. Considering the above observations, the typical sandwich-like structure is extremely consistent with our previous inference at higher temperatures. Although no proof is provided directly, Raman and SEM analyses of the steel surface can indirectly manifest the existence of sandwich-like structures for tribofilms at lower temperatures. According to previous reports, it has been recognized that the presence of Ag_2MoO_4 in tribofilms can endow composites with better tribological performance [32]. Nevertheless, it should be noted that the poor binding

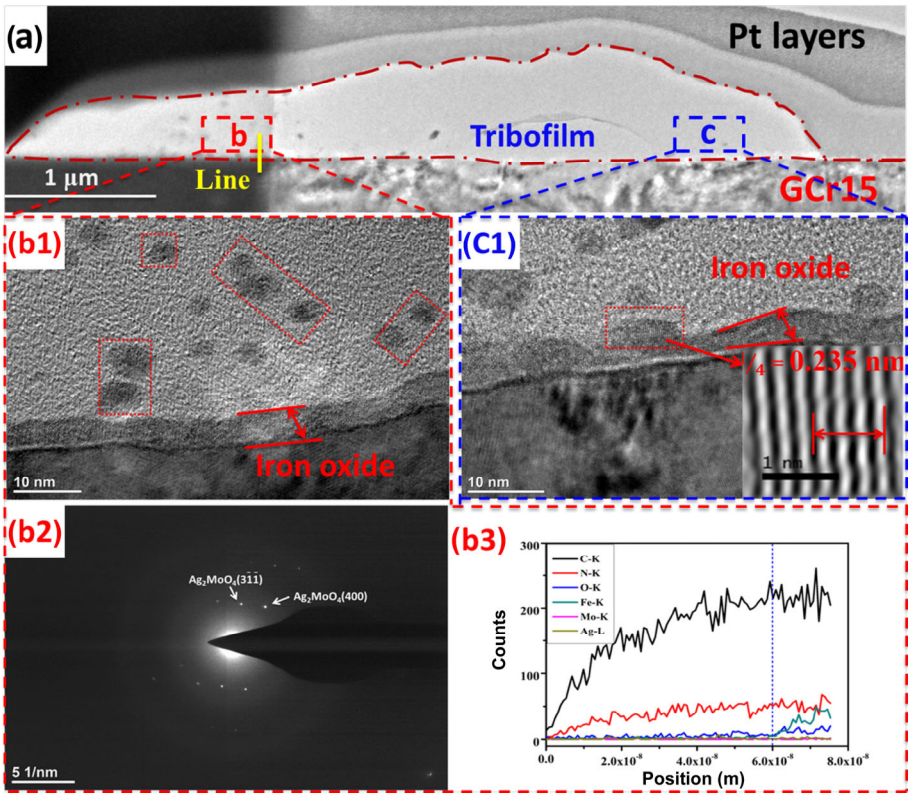

Fig. 9 (a) TEM image of the cross-section of tribofilm formed on the steel surface at 200 °C, (b1) high-magnification TEM images of zone b, (b2) the selected area electron diffraction (SAED) of zone b, (b3) EDXS line scans across zone b with a yellow line, and (c1) high-magnification TEM images of zone c.

interactions between TPI and Ag-Mo hybrids would significantly decrease this reduction, especially at higher temperatures. In addition, tribofilms are easy to break via stripped fibers when the bulk temperature is increased. It is thus inferred that the friction and wear behavior of TPI-1 is balanced by removal and replenishment of tribofilms formed by Ag-Mo hybrids.

4 Conclusions

Ag-Mo hybrids as lubricants were incorporated into a TPI matrix to successfully prepare TPI composites (TPI-1) using the conventional hot compression process. Subsequently, the friction and wear behaviors of TPI-1 were investigated at different temperatures. When the bulk temperature was below 100 °C, TPI-1 exhibited an excellent tribological performance. The TEM and EDXS characterization results demonstrated that sandwich-like tribofilms entrapped with Ag-Mo hybrids were established at different temperatures. This result indicates that friction and wear behavior of TPI-1 can be significantly improved, which is mainly attributed to the removal and replenishment of tribofilms formed by Ag-Mo hybrids.

Acknowledgements

We thank to financially supported by the National Natural Science Foundation of China-Academy of Engineering Physics Joint Fund (NSAF) (U1630128), the National Natural Science Foundation of China-Aerospace Science and Technology Corporation of China Aerospace Advanced Manufacturing Technology Research Joint Fund (U1637205), and the National Basic Research Program of China (973 Program, 2015CB057502). This work was also partially supported by the National Natural Science Foundation of China (51673205, 51565025) and the Key Research Program of Frontier Science, Chinese Academy of Sciences (Grant QYZDJ-SSW-SLH056).

References

[1] Holmberg K, Erdemir A. Influence of tribology on global energy consumption, costs and emissions. *Friction* **5**(3): 263–284 (2017)

[2] Qi H M, Li G T, Zhang G, Wang T M, Wang Q H. Impact of counterpart materials and nanoparticles on the transfer film structures of polyimide composites. *Mater Des* **109**: 367–377 (2016)

[3] Zhang G, Häusler I, Österle W, Wetzel B, Jim B. Formation and function mechanisms of nanostructured tribofilms of epoxy-based hybrid nanocomposites. *Wear* **342**–**343**: 181–188 (2015)

[4] Duan C J, Yuan D M, Yang Z H, Li S, Tao L M, Wang Q H, Wang T M. High wear-resistant performance of thermosetting polyimide reinforced by graphitic carbon nitride (g-C_3N_4) under high temperature. *Compos Part A*: *Appl Sci Manuf* **113**: 200–208 (2018)

[5] Lin L Y, Schlarb A K. The roles of rigid particles on the friction and wear behavior of short carbon fiber reinforced PBT hybrid materials in the absence of solid lubricants. *Tribol Int* **119**: 404–410 (2018)

[6] Nunez E E, Gheisari R, Polycarpou A A. Tribology review of blended bulk polymers and their coatings for high-load bearing applications. *Tribol Int* **129**: 92–111 (2019)

[7] Yu D Y, Weng L J, Ouyang J L. Recent progress of the space mechanism lubrication. *Tribology* **16**(1): 89–95 (1996)

[8] Harvey B G, Yandek G R, Lamb J T, Eck W S, Garrison M D, Davis M C. Synthesis and characterization of a high temperature thermosetting polyimide oligomer derived from a non-toxic, sustainable bisaniline. *RSC Adv* **7**(37): 23149–23156 (2017)

[9] Min C Y, Liu D D, Shen C, Zhang Q Q, Song H J, Li S J, Shen X J, Zhu M Y, Zhang K. Unique synergistic effects of graphene oxide and carbon nanotube hybrids on the tribological properties of polyimide nanocomposites. *Tribol Int* **117**: 217–224 (2018)

[10] Ma J, Qi X W, Zhao Y L, Zhang Q L, Yang Y L. Effects of elevated temperature on tribological behavior of polyimide and polyimide/mesoporous silica nanocomposite in dry sliding against GCr15 steel. *Wear* **374**–**375**: 142–151 (2017)

[11] Friedrich K. Polymer composites for tribological applications. *Adv Ind Eng Polym Res* **1**(1): 3–39 (2018)

[12] Zhang Y X, Miyauchi M, Nutt S. Structure and properties of a phenylethynyl-terminated PMDA-type asymmetric polyimide. *High Perform Polym* **31**(3): 261–272 (2019)

[13] Yu P, Wang Y, Yu J R, Zhu J, Hu Z M. Influence of different ratios of a-ODPA/a-BPDA on the properties of phenylethynyl terminated polyimide. *J Polym Res* **25**(5): 110 (2018)

[14] Chen Y, Li D X, Yang W Y, Xiao C G, Wei M L. Effects of different amine-functionalized graphene on the mechanical, thermal, and tribological properties of polyimide nanocomposites synthesized by in situ polymerization. *Polymer* **140**: 56–72 (2018)

[15] Qin S L, Cui M J, Dai Z D, Qiu S H, Zhao H C, Wang L P, Zhang A F. Noncovalent functionalized graphene-filled polyimides with improved thermal, mechanical, and wear resistance properties. *Tribol Lett* **66**(2): 69 (2018)

[16] Bijwe J, Indumathi J. Influence of fibers and solid lubricants on low amplitude oscillating wear of polyetherimide composites. *Wear* **257**(5–6): 562–572 (2004)

[17] Berman D, Erdemir A, Sumant A V. Approaches for achieving superlubricity in two-dimensional materials. *ACS Nano* **12**(3): 2122–2137 (2018)

[18] Chen B B, Li X, Jia Y H, Li X F, Yang J, Yan F Y, Li C S. MoS_2 nanosheets-decorated carbon fiber hybrid for improving the friction and wear properties of polyimide composite. *Compos Part A*: *Appl Sci Manuf* **109**: 232–238 (2018)

[19] Pan F, Wang G R, Liu L Q, Chen Y L, Zhang Z, Shi X H. Bending induced interlayer shearing, rippling and kink buckling of multilayered graphene sheets. *J Mech Phys Solids* **122**: 340–363 (2019)

[20] Xiao H P, Liu S H. 2D nanomaterials as lubricant additive: A review. *Mater Des* **135**: 319–332 (2017)

[21] Zhang Z Z, Yang M M, Yuan J Y, Guo F, Men X H. Friction and wear behaviors of MoS2-multi-walled-carbonnanotube hybrid reinforced polyurethane composite coating. *Friction* **7**(4): 316–326 (2019)

[22] Li Q, Serem W K, Dai W, Yue Y, Naik M T, Xie S X, Karki P, Liu L, Sue H J, Liang H, et al. Molecular weight and uniformity define the mechanical performance of lignin-based carbon fiber. *J Mater Chem A* **5**(25): 12740–12746 (2017)

[23] Guo L H, Qi H M, Zhang G, Wang T M, Wang Q H. Distinct tribological mechanisms of various oxide nanoparticles added in PEEK composite reinforced with carbon fibers. *Compos Part A*: *Appl Sci Manuf* **97**: 19–30 (2017)

[24] Samyn P, De Baets P, Vancraenenbroeck J, Verpoort F. Postmortem raman spectroscopy explaining friction and wear behavior of sintered polyimide at high temperature. *J Mater Eng Perform* **15**(6): 750–757 (2006)

[25] Fusaro R L. Effect of atmosphere and temperature on wear, friction, and transfer of polyimide films. *A S L E Trans* **21**(2): 125–133 (1978)

[26] Torres H, Rodríguez Ripoll M, Prakash B. Tribological behaviour of self-lubricating materials at high temperatures. *Int Mater Rev* **63**(5): 309–340 (2018)

[27] Allam I M. Solid lubricants for applications at elevated temperatures: A review. *J of Mater Sci* **26**(15): 3977–3984 (1991)

[28] Chen J, An Y L, Yang J, Zhao X Q, Yan F Y, Zhou H D, Chen J M. Tribological properties of adaptive NiCrAlY–Ag–Mo coatings prepared by atmospheric plasma spraying. *Surf Coat Technol* **235**: 521–528 (2013)

[29] Li B, Jia J H, Gao Y M, Han M M, Wang W Z. Microstructural and tribological characterization of NiAl matrix self-lubricating composite coatings by atmospheric plasma spraying. *Tribol Int* **109**: 563–570 (2017)

[30] Muratore C, Voevodin A A, Hu J J, Zabinski J S. Multilayered YSZ–Ag–Mo/TiN adaptive tribological nanocomposite coatings. *Tribol Lett* **24**(3): 201–216 (2006)

[31] Hu J J, Muratore C, Voevodin A A. Silver diffusion and high-temperature lubrication mechanisms of YSZ–Ag–Mo based nanocomposite coatings. *Compos Sci Technol* **67**(3–4): 336–347 (2007)

[32] Chen J, Zhao X Q, Zhou H D, Chen J M, An Y L, Yan F Y. HVOF-sprayed adaptive low friction NiMoAl–Ag coating for tribological application from 20 to 800℃. *Tribol Lett* **56**(1): 55–66 (2014)

[33] Zhang C W, Zheng D Z, Seo Y W, Wang L Q, Gu L. The effect of a thermal contact sensor on the temperature distribution and heat flux at the disk surface. *Tribol Int* **131**: 679–685 (2019)

[34] Duan C J, Cui Y, Wang C, Tao L M, Wang Q H, Xie H, Wang T M. High temperature tribological properties of thermosetting polyimide. *Tribology* **37**(6): 717–724 (2017)

[35] Gulbiński W, Suszko T. Thin films of MoO_3–Ag_2O binary oxides–the high temperature lubricants. *Wear* **261**(7–8): 867–873 (2006)

[36] Zhu J J, Xu M, Yang W L, Li D Y, Zhou L P, Fu L C. Friction and wear behavior of an Ag–Mo Co-implanted GH4169 alloy via ion-beam-assisted bombardment. *Coatings* **7**(11): 191 (2017)

[37] Gao L F, Wen T, Xu J Y, Zhai X P, Zhao M, Hu G W, Chen P, Wang Q, Zhang H L. Iron-doped carbon nitride-type polymers as homogeneous organocatalysts for visible light-driven hydrogen evolution. *ACS Appl Mater Interfaces* **8**(1): 617–624 (2016)

[38] Liu Y, Erdemir A, Meletis E I. A study of the wear mechanism of diamond-like carbon films. *Surf Coat Technol* **82**(1–2): 48–56 (1996)

[39] Ferrari A C. Raman spectroscopy of graphene and graphite: Disorder, electron-phonon coupling, doping and nonadiabatic effects. *Solid State Commun* **143**(1–2): 47–57 (2007)

[40] Guo L H, Li G T, Guo Y X, Zhao F Y, Zhang L G, Wang C, Zhang G. Extraordinarily low friction and wear of epoxy-metal sliding pairs lubricated with ultra-low sulfur diesel. *ACS Sustain Chem Eng* **6**(11): 15781–15790 (2018)

[41] Che Q L, Zhang G, Zhang L G, Qi H M, Li G T, Zhang C, Guo F. Switching brake materials to extremely wear-resistant self-lubrication materials via tuning interface nanostructures. *ACS Appl Mater Interfaces* **10**(22): 19173–19181 (2018)

Tingmei WANG. She is currently a researcher and doctoral supervisor at Lanzhou Institute of Chemical Physics, Chinese Academy of Sciences, China. She received her bachelor (1992) in Department of Organic Chemical Engineering, Northwest University and Ph.D. (2003) in Lanzhou Institute of Chemical Physics, Chinese Academy of Sciences. Her current research interests covered with design and preparation of porous polymer composites, design and development of polymer composites, preparation and properties of organic/inorganic nanocomposites, and development of high strength fiber reinforced composites. She has published over 130 journal papers and gained a number of awards.

Qihua WANG. He graduated from Northwestern Polytechnical University with a bachelor's degree in engineering in 1990 and a Ph.D. in Lanzhou Institute of Chemical Physics, Chinese Academy of Sciences in 1998, China. In 2004, he worked as a senior visiting scholar at the Department of Chemistry at the University of Houston, USA. He is currently a researcher and doctoral supervisor. He is the winner of the National Outstanding Youth Fund and his current research interests include composite tribology, space environmental material failure behavior and mechanism, and lubrication materials and sealing techniques under severe conditions. He has published more than 100 papers in important journals at domestic and international. As a group leader, he has undertaken more than 20 research projects.

Chunjian DUAN. He is the Ph.D. candidate in the Lanzhou Institute of Chemical Physics, Chinese Academy of Sciences, China. His research is focused on the polymer composites and its tribological performance over a wide range of temperature.